2007

Influence of microalloying precipitates on Bauschinger effect during UOE forming of line pipe steels

Andrii Kostryzhev
University of Birmingham, andrii@uow.edu.au

Martin Strangwood
University of Birmingham

Claire L. Davis
University of Birmingham

Publication Details

Kostryzhev, A. G., Strangwood, M. & Davis, C. L. (2007). Influence of microalloying precipitates on Bauschinger effect during UOE forming of line pipe steels. Materials Technology: advanced performance materials, 22 (3), 166-172.

Influence of microalloying precipitates on Bauschinger effect during UOE forming of line pipe steels

Abstract
Large diameter steel line pipes are generally produced by cold deforming hot rolled or thermomechanically controlled rolled (TMCR) plate by the three-stage 'UOE' process. Pipe strength has been found to increase or decrease relative to the plate, depending on the steel grade and plate processing history. The strength increase is due to work hardening whereas any decrease in strength arises from the Bauschinger effect due to the reverse cold deformation of the UOE process. The steel chemistry, through the presence of strengthening microalloy precipitates, and prior processing, through the size and distribution of microalloy precipitates and the presence of retained work hardening, affect the magnitude of the Bauschinger effect. In the present work, the microstructures of two microalloyed (Nb and Nb+V) steel plates have been examined in terms of their grain size distributions, microalloy precipitate type, size and volume fraction to determine the major contributions to the plate strength levels. It has been found that both steels are primarily strengthened by a combination of grain size refinement and precipitate strengthening. Compression-tension testing has been carried out to determine the Bauschinger parameters for the two steels. The Bauschinger stress parameter, defined for the yield point (0·1% of reverse deformation), was higher for the Nb+V steel (greater microalloying content) than the Nb steel. Transmission electron microscopy (TEM) investigations are being used to determine dislocation-dislocation and precipitate-dislocation interactions and how the spatial inhomogeneity in precipitate distribution affects the Bauschinger parameters.

Keywords
uoe, during, pipe, effect, line, bauschinger, influence, forming, microalloying, precipitates, steels

Disciplines
Engineering | Science and Technology Studies

Publication Details
Kostryzhev, A. G., Strangwood, M. & Davis, C. L. (2007). Influence of microalloying precipitates on Bauschinger effect during UOE forming of line pipe steels. Materials Technology: advanced performance materials, 22 (3), 166-172.

INFLUENCE OF MICROALLOYING PRECIPITATES ON BAUSCHINGER EFFECT DURING UOE FORMING OF LINE-PIPE STEELS

A. G. Kostryzhev, M. Strangwood, and C. L. Davis
Department of Metallurgy and Materials, University of Birmingham, Edgbaston, Birmingham, B15 2TT

ABSTRACT

Large diameter steel line pipes are generally produced by cold deforming hot rolled or thermomechanically controlled rolled (TMCR) plate by the three-stage 'UOE' process. Pipe strength has been found to increase or decrease relative to the plate, depending on the steel grade and plate processing history. The strength increase is due to work hardening whereas any decrease in strength arises from the Bauschinger effect due to the reverse cold deformation of the UOE process. The steel chemistry, through the presence of strengthening microalloy precipitates, and prior processing, through the size and distribution of microalloy precipitates and the presence of retained work hardening, affect the magnitude of the Bauschinger effect. In the present work, the microstructures of two microalloyed (Nb and NbzV) steel plates have been examined in terms of their grain size distributions, microalloy precipitate type, size and volume fraction to determine the major contributions to the plate strength levels. It has been found that both steels are primarily strengthened by a combination of grain size refinement and precipitate strengthening. Compression–tension testing has been carried out to determine the Bauschinger parameters for the two steels. The Bauschinger stress parameter, defined for the yield point (0.1% of reverse deformation), was higher for the NbzV steel (greater microalloying content) than the Nb steel. Transmission electron microscopy (TEM) investigations are being used to determine dislocation–dislocation and precipitate–dislocation interactions and how the spatial inhomogeneity in precipitate distribution affects the Bauschinger parameters.

Keywords: Line pipe steels, UOE process, Bauschinger effect, Microalloyed steels, Microalloy precipitates, Strengthening mechanisms

INTRODUCTION

The three-stage "UOE" forming process (see Figure 1) is utilised for the production of thick walled (6.4 mm - 50.8 mm) large diameter (400 mm - 1050 mm) welded steel pipes for the oil and gas industries [1]. This process is used for pipe forming hot-rolled or thermo-mechanically controlled rolled (TMCR) plates with strength levels up to API 5L X120 grade. The main room temperature forming operations of the process are: U-ing from plate, O-ing to form a circular cross-section, "killing" to close the plate edges before welding and expansion (E-stage) to form a final diameter after welding (Figure 1). Typical maximum strains in the wall outside or inside layer for the processing stages are: 7% for U-ing, 3% for O-ing, 1% for "killing", 1-2% for expansion. These values decrease as the wall-thickness decreases or diameter increases.

Pipe tensile properties are determined from a specimen diametrically opposite to the weld. At this position the radius after O-ing is larger than that after U-ing. "Killing" with subsequent expansion adds another stage of the reverse cold deformation. Thus, the final mechanical properties of the pipe depend on two main parameters: the TMCR plate microstructure and the reverse cold deformation during pipe forming. The plate microstructure in its turn depends on the steel composition and rolling process parameters. Work-hardening (or work-softening) during pipe forming depends on the strain level, strain direction and the steel chemistry.

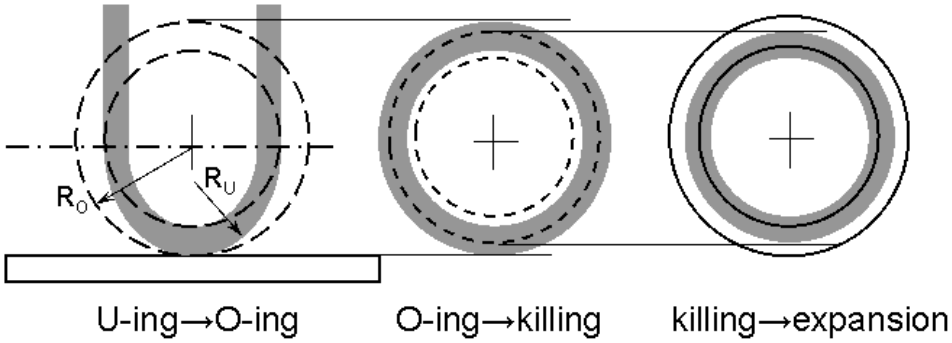

Figure 1 Schematic diagram of the UOE forming process

Severe application conditions (low temperature, high internal pressure, corrosive environment) require high strength with simultaneously high toughness for the line-pipe material. Together with the need for good weldability, this has led to decreasing carbon content and increasing microalloying element level in the steel chemistry (Table 1). The combined action of microalloying and TMCR processing results in significant grain refinement and precipitation strengthening. Introduction of accelerated cooling and decreasing finish rolling temperature gives further plate strength increases [7, 8, 9].

Table 1 Typical composition and mechanical properties of the line-pipe steel plates

Steel grade	Typical composition, wt%	Process	Mechanical properties			Ref
			Yield,MPa	UTS,MPa	CVN, J	
X60	0.12C-0.33Si-1.35Mn-0.04Nb-0.06V	TMCR	485	565		[2]
X65	0.08C-0.3Si-1.6Mn-0.08Nb-0.08V-0.017Ti-0.27Ni	TMCR	485-500	570-600	260 (-30^0C)	[3,4]
X70	0.09C-0.25Si-1.69Mn-0.05Nb-0.08V-0.003Ti-0.22Ni-0.01Mo	TMCR	500-580	600-790	200 (-10^0C)	[4]
X80	0.08C-0.4Si-1.9Mn-0.044Nb-0.019Ti-0.2Ni-0.01Mo-0.03Cr	TMCR + acc.cooling	600	730	180 (-20^0C)	[4]
X100	0.06C-0.33Si-1.95Mn-0.048Nb-0.019Ti-0.24Ni-0.3Mo	TMCR + acc.cooling	740-760	780-820	270 (-10^0C)	[5]
X120	0.05C-0.30Si-1.80Mn-0.80Cr-0.042Nb-0.017Ti-2.1Ni-0.70Mo	TMCR + acc.cooling	840-860	940-1130	260 (-30^0C)	[5,6]

Owing to cold deformation during the UOE forming strength from plate to pipe may increase or decrease. Work-hardening due to unidirectional deformation is known to be dependent on the strain level and the steel chemistry, which determines the work-hardening exponent. Reverse cold deformation, relevant to UOE forming, may result in work-softening due to the Bauschinger

effect. The Bauschinger effect in line-pipe steels has been previously observed with respect to pipe property test specimen flattening [10]. Mechanical test specimens cut from the 180^0 position to the weld and flattened showed 20% lower yield than the pipe ring hydraulic expansion test specimens [2]. Decrease in yield stress from plate to pipe during UOE forming was found to be dependent on the forming conditions, namely the strain level during the different forming stages [11], for example, with an increase in reduction after O-ing up to 1.1% the yield stress decreased by 2% in a 0.106wt%C-0.035Nb-0.035V steel. Recent study of Nb and Nb-V alloyed steel property changes from plate to pipe showed a dependence of the pipe yield stress and tensile strength on the chemical composition of the steels and plate processing history [12]. By using the back stress [13] and Orowan [14] theories of the Bauschinger effect it is possible to correlate plate to pipe property change with the dislocation structure (processing history) and microalloying precipitates (steel composition). At the moment Bauschinger parameter dependence on the dislocation structure and the steel chemistry is only known qualitatively. Thus a quantitative dependence of the Bauschinger stress parameter on the precipitate number density and dislocation density is needed. Particle volume fraction influence on the Bauschinger stress parameter has been investigated in the present paper using X60 and X65 line-pipe steel examples.

MATERIALS AND EXPERIMENTAL TECHNIQUES

Three different steel plates were provided by Corus plc, Plates and Commercial Steels (Table 2). The C-Mn plates were 8.1 mm in thickness, C-Nb 10.2 mm and C-Nb-V 10.5 mm. Mechanical properties meet the requirements of API for B grade (C-Mn), X60 (C-Nb), and X65 (C-Nb-V) (Table 3).

Table 2 Plate composition in weight %

Steel grade	C	Si	Mn	P	S	Cr	Al	Ni	Cu	Nb	V	N	Ti	Mo
C-Mn	0.12	0.23	1.09	0.019	0.100	0.023	0.33	-	0.015	0.001	0.002	0.020	0.001	0.002
C-Nb	0.10	0.37	1.36	0.012	0.006	0.017	-	0.016	0.009	0.034	0.001	0.002	0.001	0.002
C-Nb-V	0.07	0.34	1.47	0.012	0.003	0.013	-	0.021	0.015	0.046	0.061	0.004	0.002	0.002

Table 3 Plate tensile properties (courtesy of Corus)

Seel grade	YS, MPa	UTS, MPa	Elongation to failure, %
C-Mn	359	494	25
C-Nb	487	568	21
C-Nb-V	557	590	19

For *optical microscopy and image analysis* sections of approximately 10 mm x 10 mm x 10 mm in size were cut from the as-received plates, mounted in conductive bakelite parallel and perpendicular to the rolling direction, ground and polished to a 1 μm finish then etched in 2% nital.

The specimens were imaged using Leica DMRX and Zeiss Axioskop2 microscopes and analysed using KS 300 and KS 400 software. Grain size was measured as average grain diameter for 800-2000 grains and pearlite percent for 5 images at a magnification of 100x (0.161 mm^2) or 200x (0.039 mm^2) depending on the steel grade. Measurements were made across the plate thickness in 0.4 mm steps.

Scanning electron microscopy (SEM) was carried out using a Jeol JSM-7000F field emission gun scanning electron microscope. Nb- and Ti-rich precipitates were imaged from

4 regions, ferrite and pearlite, sub-surface and mid-thickness, and characterised in terms of size, morphology and area fraction. For the determination of the particle size distributions and area fraction in the C-Nb steel 630 particles from 15585 μm^2 and in the C-Nb-V steel 1064 particles from 10780 μm^2 total area were imaged.

Transmission electron microscopy (TEM) was carried out on Philips-CM20 and Philips Tecnai F20 field emission gun TEMs. V-rich particles in the C-Nb-V steel were imaged from 2 regions, plate mid-thickness and sub-surface. For the determination of the particle size distributions and volume fraction 1387 particles from 2340 nm^2 total area were imaged. Foil thickness was determined using a convergent beam diffraction technique [15].

Precipitate compositions were determined using *energy dispersive X-ray spectroscopy* (EDS) point analysis in the Jeol-6300 SEM (Noran EDS, Vantage software), Jeol-7000F SEM (Inca Oxford EDS) and Philips-CM20 TEM (Link Oxford EDS). For the Ti-, Nb- and V-rich precipitate chemical composition investigation 54 particles in the C-Nb and 65 particles in the C-Nb-V steel were used.

Compression-tension testing was carried out on an ESH 250 kN servo-hydraulic twin column low speed ramp universal testing machine. For the stress-strain curve determination 4 cylindrical specimens of 4.5 mm diameter and 13 mm gauge length were cut in the transverse orientation to the rolling direction from the C-Nb and C-Nb-V steel plates.

Thermodynamic modelling was carried out using version L of Thermo-Calc using the bulk alloy composition as an input. Equilibrium phase balances within the temperature range 600-1600 K were calculated along with phase compositions.

For ferrite *micro-hardness* distributions across the plate thickness 5 indents for each point were measured using a Shimadzu Vickers micro-hardness tester at intervals of 0.2mm., with 500 g load used.

RESULTS

Microstructure characterisation

Optical microscopy of the three steels showed banded ferrite-pearlite microstructures. The average grain size decreases with an increase of microalloying element content due to greater Zener drag and lower rolling temperatures from C-Mn to C-Nb and to C-Nb-V grades. Sub-surface plate areas showed smaller grain sizes than the mid-thickness. The second phase (pearlite) content increased towards the centreline consistent with macrosegregation. Average pearlite content decreased with decreasing carbon content. Average ferrite microhardness increases due to grain refinement and precipitation strengthening (Table 4).

Table 4 Microstructure characterisation

Steel grade	grain size, μm			pearlite content, %				Hardness HV
	sub-surface	mid-thickness	average	sub-surface	mid-thickness	average	Thermo-Calc	
C-Mn	4.0	5.3	4.65	14.3	16.3	15.3	15.0	145
C-Nb	1.8	3.1	2.45	7.0	12.2	9.6	12.1	188
C-Nb-V	1.6	3.0	2.30	3.0	6.4	4.7	6.5	194

Theoretical prediction of the carbo-nitride phase by Thermo-Calc

Thermo-Calc was used to predict the equilibrium mole fraction of microalloy carbo-nitrides with temperature (Figure 2). Larger microalloying element content leads to a larger fraction of the carbo-nitride phase in the solid state. Mole fraction of the carbo-nitride phase increases with temperature decrease as the solubility decreases. Sudden increases in mole fraction with decreasing temperature are associated with a change in the major alloying element type, e.g. from TiN to Nb (C,N).

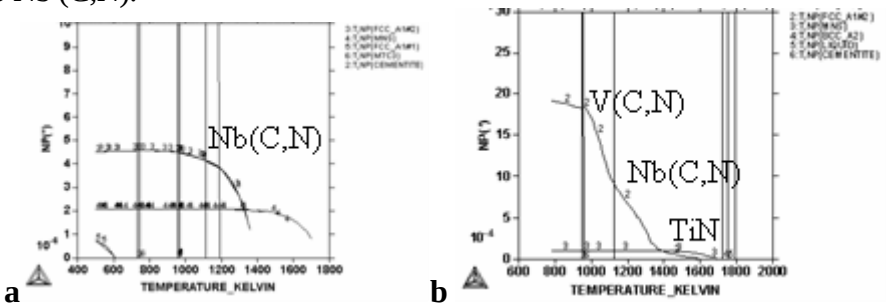

Figure 2 Thermo-Calc calculation of the carbonitride phase mole fraction versus temperature in (a) the C-Nb steel and (b) C-Nb-V steel

SEM study of Nb-rich particles

The SEM EDS of the precipitated particles in the C-Nb and C-Nb-V steels revealed these to be Nb-rich and Nb-Ti-rich (Figure 3). Particles of diameter larger than 100 nm exhibited a greater Ti level consistent with precipitation at higher temperatures giving more time for growth, than solely Nb(C,N) which formed at lower temperatures and in the solid. However, Nb and Nb-Ti containing particle average diameter and area fraction were calculated together. For the number of particles measured in this work, 630 in the C-Nb and 1064 in the C-Nb-V steel, area fraction can be considered equal to the volume fraction and compared with Thermo-Calc theoretical prediction.

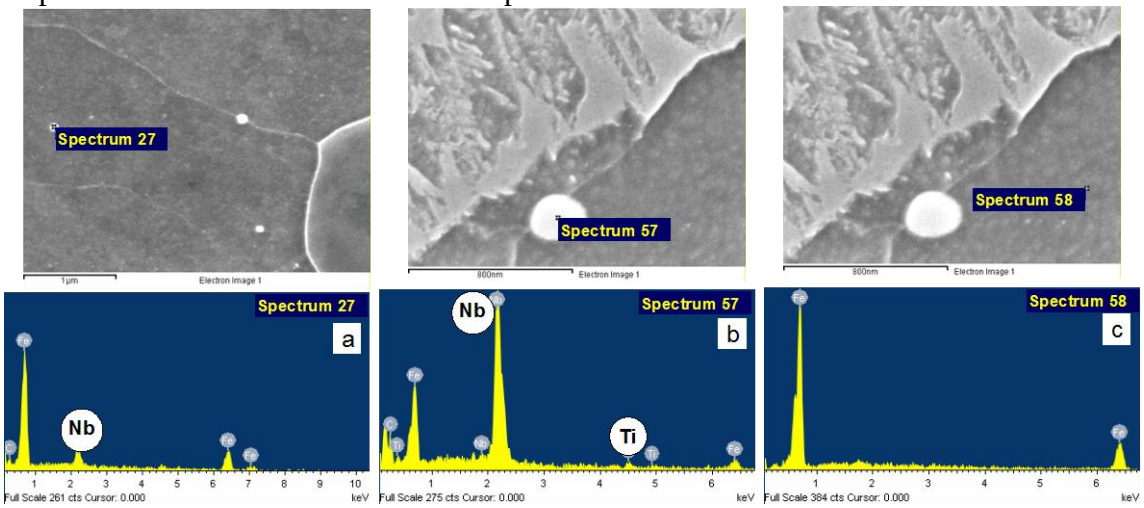

Figure 3 Typical SEM EDS spectra of (a) Nb-rich, (b) Nb-Ti-rich particles and (c) ferrite matrix in the C-Nb-V steel

Measurements of the Nb-rich particle size and volume fraction were made separately for

the ferrite and pearlite regions in sub-surface and mid-thickness areas (Figure 4, Table 5). Average particle diameter and volume fraction increase towards the mid-thickness of the plates due to macrosegregation. Volume fraction in pearlite was larger than that in ferrite due to microsegregation, consistent with previous studies [16]. Particle volume fraction increases with the increase in microalloying from the C-Nb to the C-Nb-V steel as was predicted by Thermo-Calc (Figure 2, Table 5). The smaller particle diameter observed in the C-Nb-V steel can be explained by the processing variable differences, namely lower finish roll temperature for the C-Nb-V steel (735 ^{0}C) than for the C-Nb steel (745 ^{0}C). In addition, the precipitation of V(C,N) particles takes place at lower temperatures resulting in a greater number of finer precipitates. An increase in the dislocation density with a decrease in finish roll temperature may result in an increase in precipitation number density through increased number density of nucleation sites, but this needs further investigation. Measured data for the particle volume fraction in the C-Nb steel correspond well with the Thermo-Calc calculation. In the C-Nb-V steel SEM measurements do not take into account many fine V-rich precipitates. Thus the measured value for the particle volume fraction is lower than calculated.

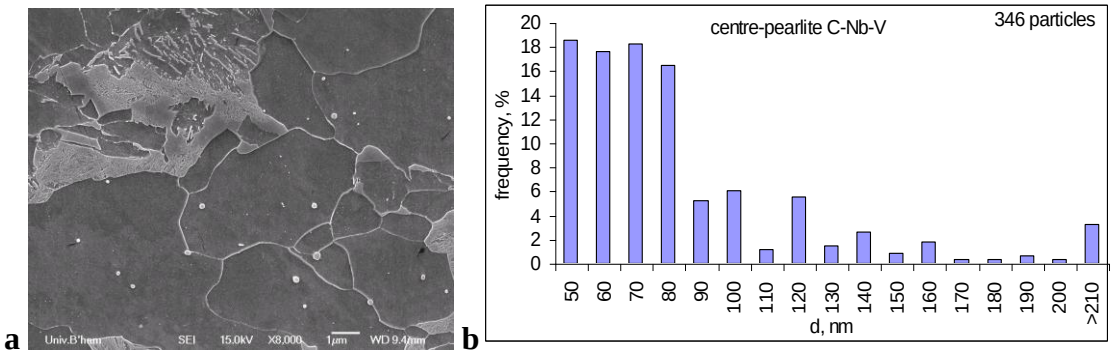

Figure 4 (a)Typical SEM image of the C-Nb-V steel mid-thickness pearlite region and (b) particle diameter frequency distribution

Table 5 Measurement results for the Nb-rich particles

Area of precipitation		average diameter, nm				volume fraction			
		C-Nb		**C-Nb-V**		**C-Nb**		**C-Nb-V**	
						f_{TC}* = 0.000365		f_{TC} = 0.001445	
sub-surface	ferrite	88	89	67	69	4.4·10-5	7·10-5	0.000372	0.000404
	pearlite	90		71		9.7·10-5		0.000476	
mid-thickness	ferrite	132	130	58	73	6.7·10-5	7·10-4	0.000165	0.000551
	pearlite	128		88		0.001325		0.000937	

*f_{TC} – particle volume fraction calculated with Thermo-Calc

TEM study of V-rich particles in C-Nb-V steel

V-rich particles were studied with TEM (Figure 5).

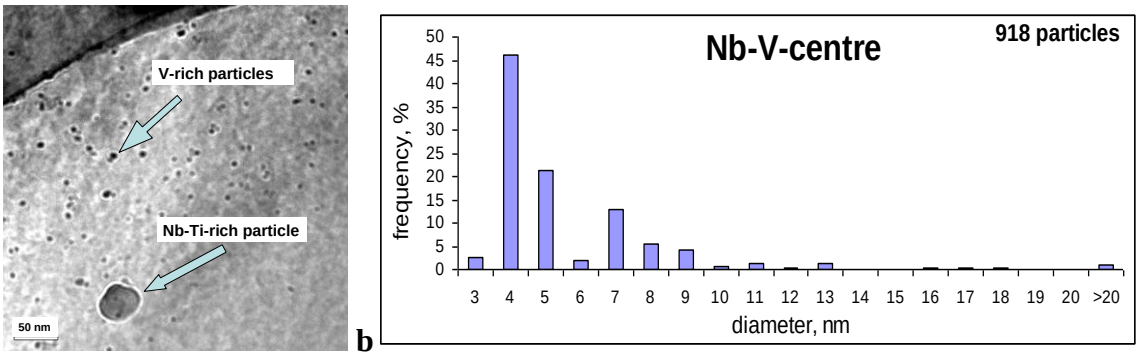

Figure 5 (a) Typical TEM image of C-Nb-V steel and (b) V-rich particle size distribution

The V-rich particles volume fraction increased from f = 0.00061 at sub-surface to f = 0.00104 at the mid-thickness position due to macrosegregation giving greater agreement with Thermo-Calc. Particle diameter was measured in the range 3 – 50 nm at the mid-thickness and 4 – 60 nm at the sub-surface position. Average particle diameter was calculated as 6 nm in the mid-thickness and 9 nm in the sub-surface areas. The decrease in particle diameter towards mid-thickness can be partially explained if an increased dislocation density gives an increased number density of nucleation sites, but this requires further investigation.

Reverse cold deformation

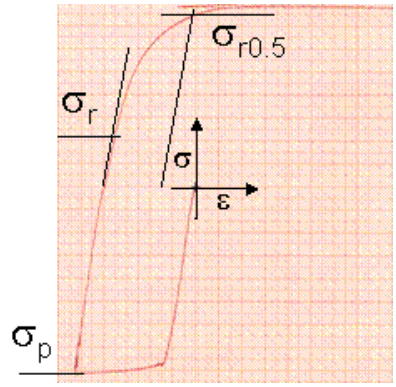

Figure 6 Typical stress-strain curve during compression-tension testing

The Bauschinger effect during cold deformation of the C-Nb and C-Nb-V steels was studied with compression-tension testing (Figure 6). Four specimens of each steel composition were compressed to different levels of pre-strain and tensile tested to failure. The Bauschinger effect was assessed by the stress parameter according to the formula [17] (Figure 6):

$$\beta_\sigma = \frac{\sigma_p - \sigma_r}{\sigma_p} \quad (1),$$

where σ_p is the maximum pre-stress and σ_r is the yield stress in the reverse direction taken at the point where the stress-strain curve deviates from the elastic deformation straight line (approximately 0.1%).

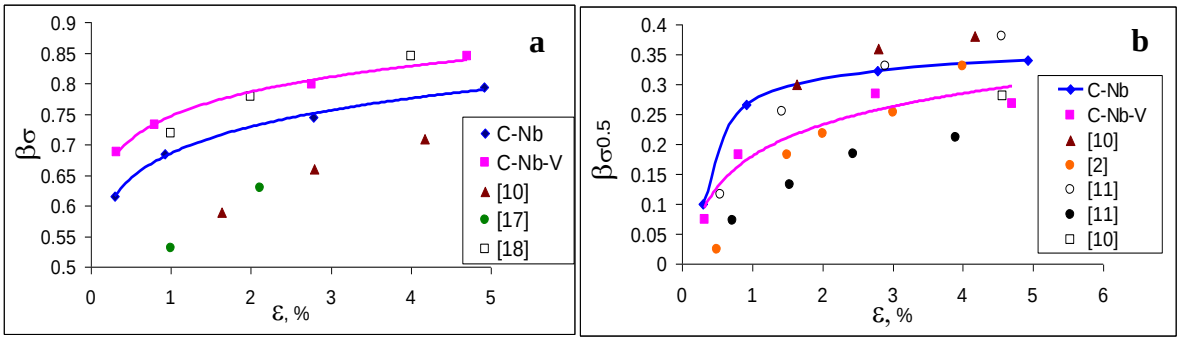

Figure 7 Bauschinger stress parameter calculated for (a) 0.1% and for (b) 0.5 % reverse strain

As prestrain and microalloying element contents increase the stress parameter increases (Figure 7,a). Equation (1) disregards work-hardening during the reverse deformation and allows assessment of the actual yield stress drop. However, in the literature, it is possible to find different expressions for the Bauschinger stress parameter [2, 10, 11, 17-19]. Thus using a different strain level for determining β_σ results in the opposite dependence on steel composition (Figure 7,b). That occurs as the work-hardening exponent increases in the reverse direction as microalloying element content increase, although the work-hardening exponent decreases with microalloying element content increase in the direction of forward deformation [12].

DISCUSSION

There are two principal Bauschinger effect theories (Figure 8); back stress and Orowan theory [13, 14]. During forward plastic deformation moving dislocations interact with different obstacles (other dislocations, grain boundaries, precipitates) preventing their further propagation. This generates a back stress around the contact point resisting further progress of similarly signed dislocations. During the reverse deformation this back stress repels the dislocations from the obstacles in the opposite direction, namely in the direction of reverse strain. Thus the stress field helps to move the dislocation in the direction of reverse strain and the reverse yield stress drops by the level of the back stress (Figure 8,a). Increase in dislocation density increases the number density of interaction sites and consequently the level of back stress. Thus the Bauschinger stress parameter is larger in steels with a higher dislocation density (larger prestrain) (Figure 7).

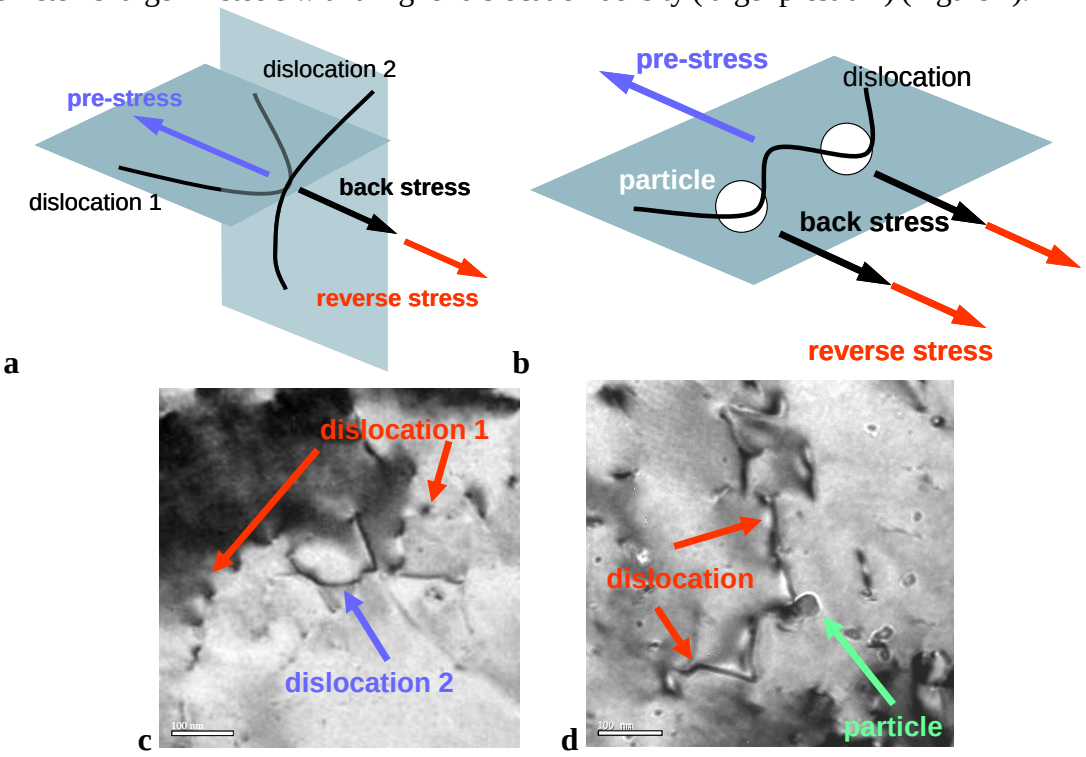

Figure 8 Schematic diagram and typical TEM micrograph of the dislocation-dislocation (a,c) and dislocation-particle (b,d) interaction

In the steels microalloyed with strong carbo-nitride forming elements precipitated particles also act as interaction sites increasing the back stress (Figure 8,b). Thus, increasing the particle volume fraction and their number density will increase the number of interactions between dislocations and particles and hence the back stress. As a result the yield stress decreases and the Bauschinger stress parameter increases with the increase in particle volume fraction (Figure 9). Based on the present work, Figure 9, the Bauschinger stress parameter, β_σ, depends on the particle volume fraction, f, as:

$$\beta_\sigma = \left(0.022 \frac{f}{10^{-4}} + 0.38 \right) \cdot \varepsilon^{0.4} + 0.61 \qquad (2),$$

where ε is the prestrain larger than 0.01.

The coefficients f and ε will depend on steel chemistry and plate processing history.

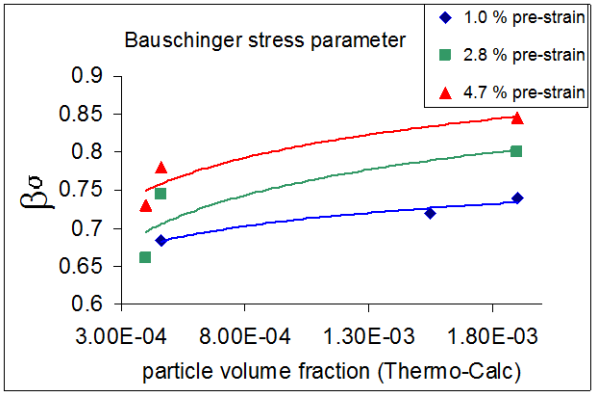

Figure 9 Bauschinger stress parameter dependence on the particle volume fraction (derived from Figure 7,a)

At present, characterisation of the dislocation structure is under way and the Bauschinger stress dependence on the dislocation density is being investigated. In future the dislocation density will be measured for the plates in the TMCR as-rolled and annealed starting conditions with respect to cold deformation strain. The aim is to correlate Bauschinger stress parameter quantitatively with the dislocation density and precipitate distribution.

CONCLUSIONS

1. In the studied microalloyed steels grain size, pearlite fraction and microalloying precipitate volume fraction and size all increase from the sub-surface to the mid-thickness of the plates.
2. Precipitate volume fraction and average size are larger in pearlite than in ferrite due to microsegregation.
3. Hardness and yield strength increased with microalloying due to grain refinement, solid solution and precipitation strengthening mechanisms.
4. An increase in prestrain increased the Bauschinger stress parameter due to the increase in dislocation density, which qualitatively corresponds with the back stress theory.
5. Quantitative dependence of the Bauschinger stress parameter on the particle volume fraction was found for the as-received steel with TMCR rolled dislocation structure.

6. Quantitative understanding of the dependence of Bauschinger stress on dislocation density requires further investigation.

Acknowledgements

The authors would like to thank Corus UK Ltd. for provision of test material. Thanks are due to the Department of Metallurgy and Materials for the provision of research facilities at the University of Birmingham. One of the authors, (AK) is grateful to 'The Universities, UK' for awarding the scholarship to carry out his research in the UK.

REFERENCES

1. www.corusgroup.com/products/tube-products/energy/linepipe (25.05.2007).
2. R.C. Ratnapuli and E.C. Rodrigues, Bauschinger effect in API X60 linepipe steels, Metals Technology, Vol. **9**, Nov., p. 440 – 445, 1982,
3. M. Gräf and H.G. Hillenbrand, Production of large diameter line pipe – state of the art and future development trends, EUROPIPE, GmbH, www.europipe.de.
4. H.G. Hillenbrand, M. Gräf and C. Kalwa, Development and production of high strength pipeline steels, EUROPIPE, GmbH, www.europipe.de, 2001.
5. H.G. Hillenbrand, C. Kalwa and A. Liessem, Technological solutions for ultra-high strength gas pipelines, EUROPIPE, GmbH, www.europipe.de, 2005.
6. H.G. Hillenbrand, A. Liessem, K. Biermann, C.J. Heckmann and V. Schwinn, Development of high strength material and pipe production technology for grade X120 line pipe, EUROPIPE, GmbH, www.europipe.de, 2004.
7. A. Streisselberger, J. Bauer, P. Flüss, H.G. Hillenbrand and P. Cordon, High strength steel plates for line pipes in grades up to X100, EUROPIPE, GmbH, www.europipe.de.
8. B. Hwang, S. Lee, Y.M. Kim, N.J. Kim and J.Y. Yoo, Correlation of rolling condition, microstructure and low temperature toughness of X70 pipeline steels, Metallurgical and Materials Transactions A, Vol. **36**, July, p. 1793 – 1805, 2005.
9. J. Bauer, P. Flüss, E. Amoris and V. Schwinn, Microstucture and properties of thermo-mechanical controlled processing steels for linepipe applications, Ironmaking and Steelmaking, Vol. **32**, №4, p. 325 – 330, 2005.
10. T.C. Harrison, R.T. Weiner and G.D. Fearnehough, Influence of the Bauschinger effect in high-yield steel pipes, Journal of Iron and Steel Institute, May, p. 334-336, 1972.
11. K. Nakajima, W. Mizutani, T. Kikuma and H. Matumoto, The Bauschinger effect in pipe forming, Transactions ISIJ, Vol. **15**, p. 1 – 10, 1975.
12. J.P. Ormandy, M. Strangwood and C.L. Davis, Effect of microalloying additions on steel plate to pipe property variations during UOE linepipe processing, Material Science and Technology, Vol. **19**, May, p. 595 – 601, 2003.
13. P.S. Bate and D.V. Wilson, Analysis of the Bauschinger effect, Acta Metallurgica, Vol. **34**, № 6, p. 1097 – 1105, 1986.
14. L.M. Brown, Orowan's explanation of the Bauschinger effect, Scripta Metallurgica, Vol. **11**, p. 127 – 131, 1977.
15. D. Williams and C.B. Carter, Transmission electron microscopy, II – Diffraction, New York, Plenum Press, 1996.

16. C.L. Davis and M. Strangwood, Preliminary study of the inhomogeneous precipitate distributions in Nb-microalloyed plate steels, Journal of Material Science, Vol. **37**, p. 1083–1090, 2002.
17. A. Abel and H. Muir, The Bauschinger effect and discontinuous yielding, Philosophical Magazine, Vol. **26**, p. 489 – 504, 1972.
18. D.N. Williams, Interaction between the Bauschinger effect and strain aging, Metallurgical Transactions A, Vol. **11**, Sept., p. 1629 – 1631, 1980.
19. R.M. Jamieson and J.E. Hood, Bauschinger effect in high-strength low-alloyed steels, Journal of Iron and Steel Institute, Jan., p. 46 – 48, 1971.